


AUTHOR QUERY FORM

	<p>Journal: Struct. Dyn.</p> <p>Article Number: 016591SDY</p>	<p>Please provide your responses and any corrections by annotating this PDF and uploading it to AIP's eProof website as detailed in the Welcome email.</p>
---	--	--

Dear Author,

Below are the queries associated with your article; please answer all of these queries before sending the proof back to AIP.

Article checklist: In order to ensure greater accuracy, please check the following and make all necessary corrections before returning your proof.

1. Is the title of your article accurate and spelled correctly?
2. Please check affiliations including spelling, completeness, and correct linking to authors.
3. Did you remember to include acknowledgment of funding, if required, and is it accurate?

Location in article	Query / Remark: click on the Q link to navigate to the appropriate spot in the proof. There, insert your comments as a PDF annotation.
AQ1	Please check that the author names are in the proper order and spelled correctly. Also, please ensure that each author's given and surnames have been correctly identified (given names are highlighted in red and surnames appear in blue).
AQ2	We have changed "billion" as "10 ⁹ ." Please check.
AQ3	Please verify the edit made in the sentence beginning "would be noted that..."
AQ4	Please verify the edits made in the sentence beginning "Since the quantities $B_l(q, q')$..."
AQ5	Please verify the edits made in the reprint credit line.
AQ6	Please provide year in Ref. 8.

Thank you for your assistance.

Use of triple correlations for the sign determinations of expansion coefficients of symmetric approximations to the diffraction volumes of regular viruses 1 2 3

AQ1 **H. C. Poon and D. K. Saldin^{a)}** 4
Department of Physics and Laboratory for Surface Studies, University of Wisconsin Milwaukee, P.O. Box 413, Milwaukee, Wisconsin 53201, USA 5
6

(Received 27 February 2015; accepted 2 June 2015; published online xx xx xxxx) 7

AQ2 An X-ray free electron laser is a new source of x-rays some 10×10^9 times 8
 brighter than any previous X-ray source, giving rise to the possibility of structure 9
 determination of individual biological particles without crystallization. Some of 10
 the earliest samples used in the X-ray free electron laser are viruses because they 11
 are about the largest of reproducible bioparticles. We show how common virus 12
 near-symmetries can be exploited to find a first approximation to their structures 13
 to give a starting point for a perturbation approach to determine their structures. 14
 © 2015 Author(s). All article content, except where otherwise noted, is licensed 15
 under a Creative Commons Attribution 3.0 Unported License.
[\[http://dx.doi.org/10.1063/1.4922476\]](http://dx.doi.org/10.1063/1.4922476)

I. INTRODUCTION 15

As demonstrated in a recent experiment,¹ a single virus particle may be injected into a 16
 very short and bright pulsed beam from a coherent X-ray free electron laser (XFEL) and is ca- 17
 pable of diffracting enough intensity to form a high-quality diffraction pattern before suffering 18
 significant damage.² Experiments have suggested the feasibility of this approach for both single 19
 particles³ and nanocrystals.⁴ Therefore, a stream of particles can be directed into an XFEL 20
 beam, and diffraction patterns recorded sequentially, each corresponding to a different particle 21
 orientation. There have also been other significant applications of XFEL radiation, such as the 22
 discovery from wide-angle X-ray scattering (WAXS) of a “protein quake” that might explain 23
 the utilization of solar energy during photosynthesis.⁵ Here, we develop a method to recover 24
 the 3D structure of a particle without knowing orientation of the particle contributing to each 25
 diffraction pattern. Though the method we describe assumes a form of symmetry (icosahedral 26
 or helical) suggested by Caspar and Klug⁶ to be usual with regular viruses, we acknowledge 27
 that many viruses deviate from this symmetry with their internal genetic material¹ or with 28
 external features such as spikes⁷ or hair.¹ Icosahedral or helical symmetry often remains 29
 the symmetry associated with the bulk of the capsid. For example, the low-resolution image of the 30
 capsid in Fig. 3 of Ref. 1 appears to be largely icosahedral with little evidence of the hair that 31
 is known to cover this virus. This suggests that a symmetric structure like those deduced here 32
 from simulated XFEL data may form an excellent first guess to such a structure which can later 33
 be modified by a form of perturbation theory as used in quantum mechanics, or else form an 34
 excellent support as a starting point in an iterative algorithm⁸ that constrains the reciprocal 35
 space data to the measured angular correlations, and the real-space image to a dynamic support 36
 based on the shrink-wrap algorithm⁹ with no symmetry restrictions. Our approach in our earlier 37
 paper¹⁰ was to find the optimum set of coefficients that ensured positivity of the diffraction 38
 intensities. This is not a very strong constraint, and there are a variety of combinations of signs 39
 which are consistent with this constraint. A stronger constraint and one which tends to 40

^{a)} Author to whom correspondence should be addressed. Electronic mail: dksaldin@uwm.edu



determine these signs more uniquely is that which makes them agree with the magnitudes and signs of the triple correlations¹¹ derived from the ensemble of diffraction patterns. In this paper, we derive precise expressions for these triple correlations in terms of the relevant expansion coefficients of the diffraction volume, and show how this constraint may be used for determining the signs of the expansion coefficients in the cases of both icosahedral and helical symmetry. The resulting 3D diffraction volume can be phased iteratively with algorithms like charge flipping^{12,13} or standard fiber diffraction phasing algorithms (e.g., Refs. 14 and 15) in the case of a helical virus.

II. AVERAGE ANGULAR CORRELATIONS

For a set of experimental diffraction patterns, the average pair correlation function may be defined by

$$C_2(q, q'; \Delta\phi) = \langle \int I(q, \phi) I(q', \phi + \Delta\phi) d\Delta\phi \rangle_{DP}, \quad (1)$$

AQ3

where q and q' refer to two resolution shells, which can be identified with concentric circles on individual diffraction patterns, and $\langle \dots \rangle_{DP}$ refers an average over diffraction patterns. It would be noted that the angular correlations themselves (Eq. (1)) are between intensities on the same diffraction patterns, and thus insensitive to shot-to-shot intensity variations, a problem with an X-ray laser. Of course, $\langle \dots \rangle_{DP}$ invokes an average over different diffraction patterns. However, such an average is much less sensitive to shot-to-shot variations than correlations between different diffraction patterns. All that is required is a reasonable statistical distribution of the shot-to-shot intensity variations. It should perhaps be pointed out that this method of determining a diffraction volume from random particle orientations works from averages over all particle orientations, and at no stage involves the determination of the relative orientations of the particles contributing to the individual diffraction patterns.

It can be shown that, in terms of the spherical harmonic expansion coefficients $I_{lm}(q)$ of the diffraction volume, this angular correlation reduces to^{16,17}

$$C_2(q, q'; \Delta\phi) = \frac{1}{4\pi} \sum_l B_l(q, q') P_l(\cos \Delta\theta), \quad (2)$$

which is independent of ϕ , where

$$B_l(q, q') = \sum_m I_{lm}^*(q) I_{lm}(q'), \quad (3)$$

and

$$\cos(\Delta\theta) = \cos(\theta(q)) \cos(\theta(q')) + \sin(\theta(q)) \sin(\theta(q')) \cos(\Delta\phi), \quad (4)$$

where $\theta(q)$ and $\theta(q')$ refer to scattering angles of the incident radiation corresponding to the resolution shells q and q' . Note that, in the above equations, the quantity B_l , which is easily recoverable from the set of measured diffraction patterns using the orthogonality property of Legendre polynomials, is a quadratic function of the spherical harmonic expansion coefficients $I_{lm}(q)$. If the expansion coefficients could be recovered directly, it would be possible to reconstruct that diffraction volume *via*

$$I(q, \phi) = \sum_{lm} I_{lm}(q) Y_{lm}(\theta(q), \phi). \quad (5)$$

Unfortunately, the quantities $B_l(q, q')$, in general, do not determine the coefficients $I_{lm}(q)$ uniquely.^{16,17} For example, the coefficients depend on the extra magnetic quantum number m ,

not specified by B_l . However, for particles of known symmetry, each l quantum number may be associated with known values of m in some known ratio. As we show below, this is certainly true of icosahedral and helical viruses. Under such circumstances, as we show below, it is possible to extract the $I_{lm}(q)$ coefficients from the measured $B_l(q, q')$.

We begin by considering the icosahedral case.

III. ICOSAHEDRAL PARTICLE

AQ4

The recovery of charge density of icosahedral virus from pair angular correlation has been reported in a previous work.¹⁰ Since the quantities $B_l(q, q')$ extractable from the pair correlations depend only on the angular momentum quantum number, l , the use of icosahedral harmonics (which also depend on the same quantum numbers as they are sums over spherical harmonics of magnetic quantum numbers m in a known proportion) allows their magnitudes to be determined by these quantities alone. Although icosahedral harmonic expansion coefficients for real intensities are real, also there remains an ambiguity of sign. In our previous work,¹⁰ we determined these signs by a positivity constraint on the intensities. This is not a very strong constraint and does not always determine the signs of the icosahedral harmonic expansion coefficients uniquely. We hereby describe an alternative, and stricter, way of constraining these signs by adjusting them to agree with the magnitudes and signs of the triple angular correlations.¹¹ As we will see, this approach is equally applicable to the great classes of virus symmetry, noted by Caspar and Klug.⁶ Icosahedral harmonics, \mathcal{I}_l , are defined by

$$\mathcal{I}_l(\theta, \phi) = \sum_m a_{lm} Y_{lm}(\theta, \phi), \quad (6)$$

where the a_{lm} are a set of known coefficients, tabulated as in, e.g., Ref. 18. A general diffraction volume of icosahedral symmetry can be described by an expansion of the form

$$I(\mathbf{q}) = \sum_l g_l(q) \mathcal{I}_l(\theta, \phi), \quad (7)$$

where the amplitudes $g_l(q)$ denote the precise combinations of the different icosahedral harmonics needed to specify the 3D diffraction volume of each particle. The quantities $g_l(q)$ only depend on l and q , precisely the parameters specifying the quantities $B_l(q, q')$ determinable by experiment.

Indeed, in terms of the quantities $g_l(q)$, it is easy to see that

$$B_l(q, q') = g_l(q) g_l(q'). \quad (8)$$

Consequently, the magnitudes of the $g_l(q)$ coefficients may be determined from the shell-diagonal parts of B_l via

$$|g_l(q)| = \sqrt{B_l(q, q)}. \quad (9)$$

Although icosahedral harmonics are known to be real and consequently the expansion coefficients $g_l(q)$ may be chosen to be real to represent a real diffraction volume, there is still an uncertainty of sign. Fortunately, it is possible to determine these signs from other quantities determinable from the experimental data, namely, the triple angular correlations defined by¹¹

$$C_3(q, q'; \Delta\phi) = \langle (I(q, \phi))^2 I(q', \phi + \Delta\phi) \rangle_{DP}. \quad (10)$$

It should be noted that these two-point triple correlations consist of functions of the products of only two pixel intensities, and consequently on averaging over perhaps a million diffraction patterns is likely to give converged values from XFEL diffraction patterns of typical proteins. The

current application is to an entire virus, which is perhaps two orders of magnitude larger than a typical protein, so the problem of weak scattered intensities probably does not arise. It can be shown that¹⁶ this can be written as

$$C_3(q, q'; \Delta\phi) = \sum_l T_l(q, q') P_l(\cos(\Delta\theta)). \tag{11}$$

In this case,

$$T_l(q, q') = \sum_{l_1 l_2} b(l_1, l, l_2) g_{l_1}(q) g_l(q') g_{l_2}(q), \tag{12}$$

where

$$b(l_1, l, l_2) = \sum_{m_1 m m_2} G(l_1, m_1, l, m, l_2, m_2) a_{l_1 m_1} a_{l m} a_{l_2 m_2}. \tag{13}$$

Here, $G(l_1, m_1, l, m, l_2, m_2)$ is a coefficient defined by

$$G(l_1, m_1, l, m, l_2, m_2) = \int Y_{l_1 m_1}(\Omega) Y_{l m}^*(\Omega) Y_{l_2 m_2}(\Omega) d\Omega. \tag{14}$$

It should be noted that T_l may be extracted from the measurable quantities C_3 as before, using the orthogonality property of Legendre functions. We may write

$$I_{lm}(q) = a_{lm} g_l(q), \tag{15}$$

where $g_l(q)$ is real function of q , and a_{lm} is real. In Eq. (5), $I_{lm}(q)$ is the expansion coefficient with respect to complex spherical harmonics. It is different from most previous works which expand intensity in terms of real spherical harmonics.¹⁰ In Eq. (15), a_{lm} is related to the tabulated values a_{lm}^{IH} of Ref. 18 by

$$a_{lm} = \frac{\frac{a_{lm}^{IH}}{2}}{\sqrt{\sum_m \left(\frac{a_{lm}^{IH}}{2}\right)^2}}. \tag{16}$$

The z axis has been chosen to be along a five-fold axis of the icosahedron, and the zx plane chosen along a mirror plane cutting the pentagon in the xy plane between two vertices. Such a choice ensures that all quantities in Eq. (15) are real. Note that the real square root in Eq. (9) exists because $B_l(q, q)$ is real by the definition in Eq. (3). In a previous work,¹⁰ we determine the signs of $g_l(q)$ by the positivity condition of intensity. Here, we will make use of the triple correlation which in general provides a more stringent condition on the signs. Because of Friedel's rule,

$$I(-\vec{q}) = I(\vec{q}), \tag{17}$$

l must be even. The simple form in Eq. (15) is valid only for $l < 30$, and a_{lm} is non-zero only for selected values of l .¹⁸ The allowed even values of l for non-degenerate icosahedral harmonics are 0, 6, 10, 12, 16, 18, 20, 22, 24, 26, and 28. For a given shell, specified by a value of q , the number of possible combinations of the signs of g_l is $2^{11} = 2048$. We can determine these signs by an exhaustive search over all possible combinations of signs in order to fit $T_l(q, q)$ in Eq. (12). By means of Eq. (8),

$$g_l(q) = \frac{B_l(q, q_{ref})}{g_l(q_{ref})}. \tag{18}$$

This relation can be used to propagate the signs from the reference shell $q = q_{ref}$ to other shells, characterized by a general q . However, numerical instability may occur if $g_l(q_{ref})$ in Eq. (18) is close to zero. This instability can be overcome by taking multiple shells q as the reference shell. For each l , we can go through all shells to pick out the one with the largest magnitudes of $g_l(q)$. That shell is then used as the q_{ref} for that particular l . To demonstrate this method, simulated experimental data for B and T were obtained directly from the Protein Data Bank (PDB) file of the icosahedral virus Paramecium bursaria Chlorella virus (PBCV-1). The sign combinations which give the best fit between the theoretical (Eq. (12)) and experimental (Eq. (11)) shell-diagonal components of T for all the reference shells were found. The signs can then be propagated to other shells using the chosen multiple references by the non-shell-diagonal B 's. With all the signs determined, the $I_{lm}(q)$ and hence the diffraction volume can be calculated. The flipping method^{12,13} was used for phasing the diffraction volume to give the charge density of PBCV-1 shown in Fig. 1. Since $l_{max} = q_{max} \times R$, where $R = 1000 \text{ \AA}$, is the radius of the virus, and $l_{max} = 28$ for PBCV-1, we have $q_{max} = 28/1000 = 0.028 \text{ \AA}^{-1}$. Therefore, this method is restricted to a resolution of $2\pi/q_{max}$ or 220 \text{ \AA}. Fig. 1 was calculated for this resolution. As expected, it is icosahedrally symmetric.

The degeneracy of icosahedral harmonics for l between 30 and 44 is only two-fold.¹⁹ Between $l = 30$ and $l = 44$, therefore, one may write

$$B_l(q, q') = \sum_{n, n'=1}^2 g_{nl}(q) O_{nn'} O_{n'n}^T g_{nl}(q'), \quad (19)$$

where the matrix O and its transpose O^T are single parameter (2×2) orthogonal matrices that cannot be determined by B_l alone since $OO^T = I$, where I is the identity matrix. However, they can be determined by an optimization algorithm from the triple correlations $T_l(q, q')$, where they appear in triplicate and therefore do not cancel. Further work is in progress on this idea. Although to achieve even higher resolution would require the use of many-fold degenerate icosahedral harmonics, there do not, in principle, seem to be reasons they cannot also be found by such techniques, because all the q cross-diagonal T_l 's can be determined by this technique from experimental data. To put it another way, although there are extra parameters specified by the extra quantum number n specifying the degenerate icosahedral harmonics, we can also exploit the extra information in the q off-diagonal triple correlations $T_l(q, q')$ which we do not exploit currently. In other words, we are currently using only a fraction of the data available to us by working only with the q diagonal values of the T_l quantities.

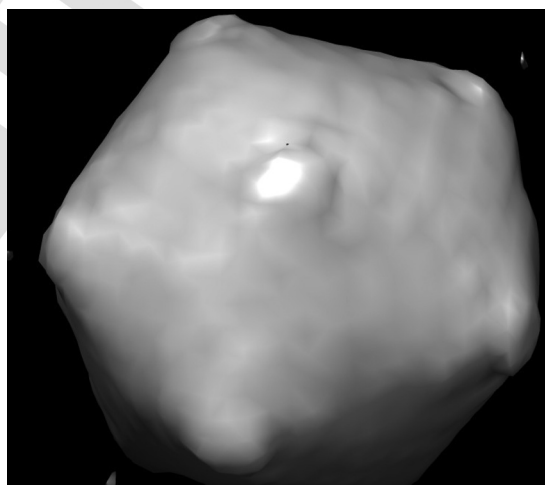


FIG. 1. Charge density of Chlorella by flipping algorithm applied to the diffraction volume determined as described from quantities extractable from angular correlations of the intensities of XFEL diffraction patterns.

IV. HELICAL VIRUS

164

By the theory of Cochran, Crick, and Vand (CCV), a helix with u subunits or proteins per period should have an integral multiple of u -fold azimuthal symmetry,^{20,21} For the tobacco mosaic virus (TMV) with a radius of 100 \AA , $u = 49$. For a resolution of 12 \AA , $l_{max} = 48$. Therefore, only zero-fold or azimuthal symmetry is possible below this resolution. Consequently, only the $m = 0$ term exists in Eq. (3), which reduces to

$$B_l(q, q') = I_{l0}(q)I_{l0}(q'). \tag{20}$$

From Eq. (20), we have

170

$$I_{l0}(q) = \text{sgn}(q, l) \sqrt{B_l(q, q)}, \tag{21}$$

which has exactly the same form as in the icosahedral case except now the angular momentum goes up to 48, and we have a much larger number of possible sign combinations. Again, we make use of triple correlation to determine the signs. The theoretical expression for the triple correlations may be written

171

172

173

174

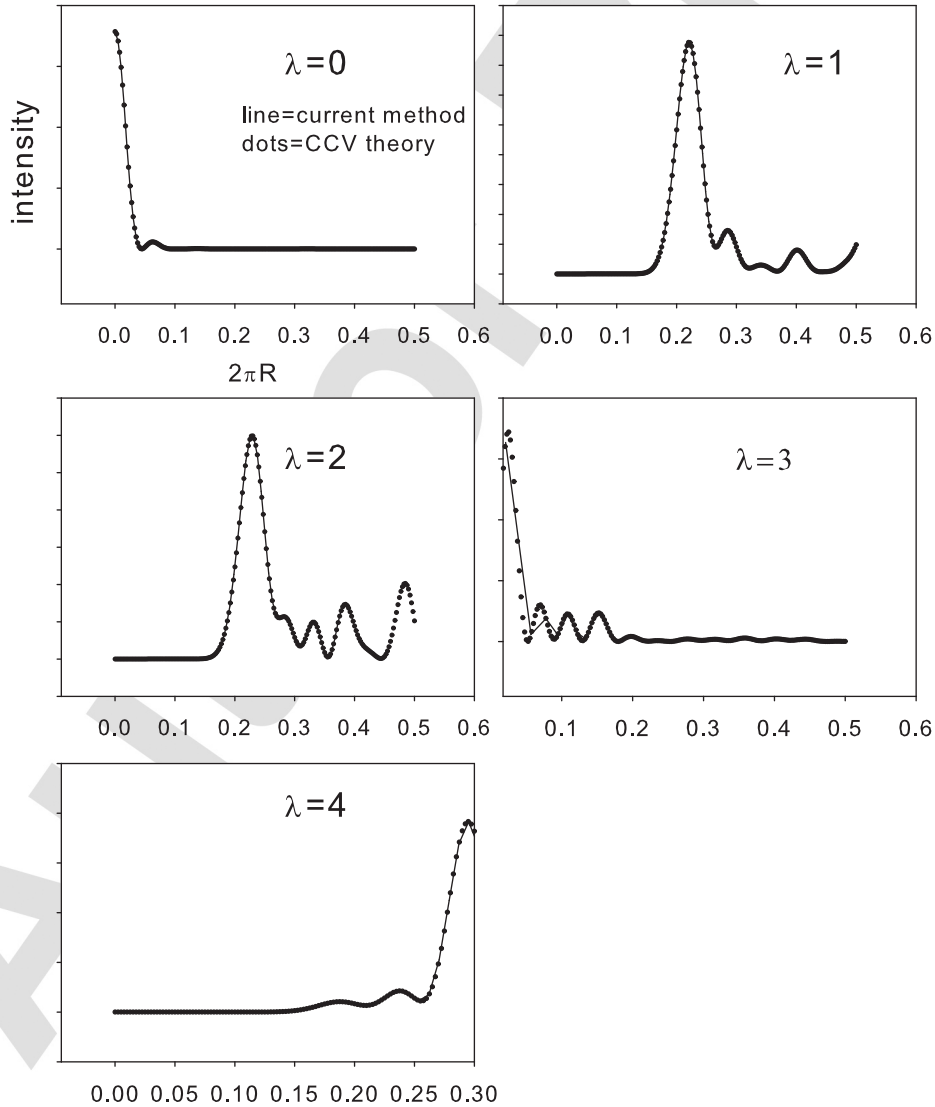


FIG. 2. Fiber diffraction intensity versus radial wave vector. Line is from current theory. Dots from CCV theory. λ is the layer line index with the wave vector component along the axis $q_z = \lambda 2\pi/c$, where c is the period of the helix.

$$T_l(q, q') = \sum_{l_1 l_2} G(l_1, 0, l, 0, l_2, 0) I_{l_1,0}(q) I_{l_2,0}(q') I_{l,0}(q). \quad (22)$$

To demonstrate this method, the simulated experimental data for B and T of TMV were 175
 obtained directly from CCV theory. In this case, since the number of sign combinations is too 176
 large for an exhaustive search, we use simulated annealing (SA) method instead to minimize 177
 the difference between theoretical and experimental triple correlations on a reference shell. In 178
 the case of helical virus, it turns out that the magnitude of $I_{l_0}(q)$ does not decay rapidly as a 179
 function of l . Therefore, any shell can be chosen as reference shell without causing numerical 180
 instability. The SA algorithm was started with a sufficiently high temperature with a high 181
 acceptance rate (about 97%) and a random sign combination $sgn(q_{ref}, l)$ at a reference shell; 182
 the temperature was then slowly decreased with a cooling rate of 0.9. Each sign at temperature 183
 T was flipped one at a time, and the new configuration was always accepted if the energy pa- 184
 rameter decreases or ΔR was negative. In the present case, ΔR is defined as the change of R 185
 factor between theoretical and experimental (q diagonal) triple correlations at $q = q_{ref}$. On the 186
 other hand, if the energy increases or ΔR is positive, the configuration is accepted with a proba- 187
 bility $e^{-\Delta R/T}$ according to the Metropolis criterion.²² At each temperature, 500 initial sweeps 188
 were performed on all signs to thermalize the system. Each sweep consists of successive flips 189
 over all the signs. Then 500 additional sweeps were performed and the R factors sampled and 190
 averaged. The temperature was lowered, and the same procedure was repeated until the accep- 191
 tance rate is very low or the average R factor stayed constant for 4 successive temperatures. 192

The final optimized combination of signs was used to find the $I_{l_0}(q)$'s at the reference 193
 shell. Again, after the optimum sign combination was found by triple correlation on a reference 194
 shell, the signs were propagated to other shells by the non-diagonal pair correlation matrix 195

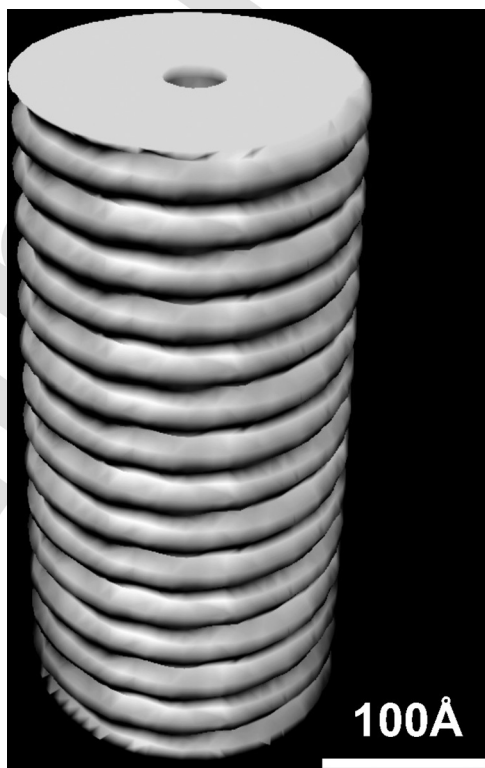


FIG. 3. Real space image reconstructed from the quantities B and T capable of being recovered from XFEL diffraction patterns of randomly oriented particles in SO(3) by assuming $m = 0$ for the layer line intensities. The reconstructed image of a single unit cell was then repeated five times along the c -axis to produce this image. Reprinted with permission from H.-C. Poon *et al.*, Phys. Rev. Lett. **110**, 265505 (2013). Copyright 2013 American Physical Society.

AQ5

$B_l(q, q')$ in Eq. (20). Having thus obtained the signs of the $I_{l0}(q)$ coefficients in addition to their magnitudes, the diffraction volume was calculated by

$$I(q, \theta) = \sum I_{l0}(q) P_l(\cos(\theta)). \quad (23)$$

The comparison between this recovered intensity and original CCV intensity along the layer lines is shown in Fig. 2. This was found to consist of some discrete layer planes perpendicular to the helical axis (q_z axis) at positions $q_z = \lambda 2\pi/c$, where $\lambda = 0, 1, 2$, etc., and c is the period as expected from fiber diffraction. As the recovered intensity along the layer lines is the same as that in conventional fiber diffraction experiment, the standard fiber diffraction methods for phasing fiber diffraction intensity can be applied to obtain the structure of TMV.

Finally, the real space image Fig. 3 was reconstructed as described in the caption from a diffraction volume of a single c -repeat unit and repeated 5 times to produce an image from a 5-unit virus, by repeating the image 5 times to produce a 5 c -repeat unit structure. We reconstructed a real-space image from this diffraction volume with the same flipping algorithm that we used for the icosahedral virus. It should be pointed out that methods of fiber diffraction have perfected over the years methods of reconstructing a real-space structure from the layer-line intensities. Therefore, it is sufficient for us to reconstruct the correct layer-line intensities by this method to enable “fiber diffraction without fibers”.

V. CONCLUSION

We have shown that for molecules with either icosahedral or helical symmetry, the symmetries of near-symmetries associated with almost all regular viruses, the spherical harmonic components of the intensity can be obtained directly up to a sign from the pair correlations B . In order to resolve the sign ambiguity, the triple correlations of the experimental intensities are exploited. For the helical TMV, we demonstrated how the fiber diffraction intensity can be recovered without the need for aligning the randomly orientated fibers by experimental means. In both cases, a reconstructed real-space image was obtained by an iterative phasing algorithm applied to the recovered diffraction volume.

ACKNOWLEDGMENTS

We acknowledge support for this work from a National Science Foundation Science and Technology Center (NSF Grant No. 1231306).

¹T. Ekeberg *et al.*, *Phys. Rev. Lett.* **114**, 098102 (2015).

²R. Neutze *et al.*, *Nature* **406**, 752 (2000).

³H. N. Chapman *et al.*, *Nat. Phys.* **2**, 839 (2006).

⁴H. N. Chapman *et al.*, *Nature* **470**, 73 (2011).

⁵D. Armlund *et al.*, *Nat. Methods* **11**, 923 (2014).

⁶D. L. D. Caspar and A. Klug, *Cold Spring Harbor Symp. Struct. Biol.* **27**, 1 (1962).

⁷M. V. Cherrier *et al.*, *Proc. Natl. Acad. Sci. USA* **106**, 11085 (2009).

⁸J. J. Donatelli, P. H. Zwart, and J. A. Sethian, private communication (■).

⁹S. Marchesini *et al.*, *Phys. Rev. B* **68**, 140101 (2003).

¹⁰D. K. Saldin, P. Schwander, H. C. Poon, M. Uddin, and M. Schmidt, *Opt. Express* **19**, 17318 (2011).

¹¹Z. Kam, *J. Theor. Biol.* **82**, 15 (1980).

¹²G. Oszlányi and A. Süto, *Acta Crystallogr., A* **60**, 134 (2004).

¹³G. Oszlányi and A. Süto, *Acta Crystallogr., A* **61**, 147 (2005).

¹⁴K. Namba and G. Stubbs, *Science* **231**, 1401 (1986).

¹⁵R. Pattanayek and G. Stubbs, *J. Mol. Biol.* **228**, 516 (1992).

¹⁶Z. Kam, *Macromolecules* **10**, 927 (1977).

¹⁷D. K. Saldin, V. L. Shneerson, R. Fung, and A. Ourmazd, *J. Phys. Condens. Matter* **21**, 134014 (2009).

¹⁸A. Jack and S. C. Harrison, *J. Mol. Biol.* **99**, 15 (1975).

¹⁹Y. Zheng and P. Doerschuk, *Siam J. Math. Anal.* **32**, 538 (2000).

²⁰H. C. Poon, P. Schwander, M. Uddin, and D. K. Saldin, *Phys. Rev. Lett.* **110**, 265505 (2013).

²¹W. Cochran, F. H. Crick, and V. Vand, *Acta Crystallogr.* **5**, 581 (1952).

²²N. Metropolis, A. W. Rosenbluth, M. N. Rosenbluth, A. H. Teller, and E. Teller, *J. Chem. Phys.* **21**, 1087 (1953).

AQ6